Korean J. Chem. Eng., 38(3), 576-586 (2021)
DOI: 10.1007/s11814-020-0712-1

pISSN: 0256-1115
eISSN: 1975-7220

Ethylene/propylene separation using mixed matrix membranes of poly (ether block amide)/nano-zeolite (NaY or NaA)

Xi Zhang*, Mengyu Yan*, Xianshe Feng, Xiaodong Wang*,†, and Wei Huang*,†**

*Key Laboratory of Coal Science and Technology of Ministry of Education and Shanxi Province, Taiyuan University of Technology, Taiyuan 030024, Shanxi, China
**Department of Chemical Engineering, University of Waterloo, Waterloo, Ontario, Canada N2L 3G1
(*Received 8 June 2020 • Revised 13 October 2020 • Accepted 16 November 2020*)

Abstract−Generally, the energy and capital intensive cryogenic distillation process is applied to separate light olefins. To lower the cost of light olefin production, mixed matrix membranes (MMMs) incorporating nano-zeolite (NaY or NaA) into a rubbery poly (ether block amide) (PEBA 2533) were fabricated to separate a propylene/ethylene mixture. The effect of additive content and kind, MMM thickness, and operating temperature and pressure on the separation performance of the synthesized membranes for a propylene/ethylene mixture were investigated. As an additive, NaY was found to be more effective than NaA. Interestingly, the result of pure gas adsorption was consistent with the permeation performance of the membranes. Membranes with 6 wt% NaY showed the highest C_3H_6/C_2H_4 selectivity in all synthesized membranes (3 wt%-10 wt%), on which, the C_3H_6/C_2H_4 selectivity was increased from 2.3 to 13.1, the permeability of propylene increased from 194 barrer to 262 barrer and the permeability of ethylene decreased from 85 barrer to 19.8 barrer when the propylene concentration in feed mixture increased from 10 mol% to 80 mol% at −35 °C and 0.2 MPa. This membrane has the potential to separate propylene and ethylene in industry, and this work will push forward the membrane separation process for olefin production.

Keywords: Mixed Matrix Membrane, NaY Zeolite, NaA Zeolite, PEBA2533, Propylene/Ethylene Mixture

INTRODUCTION

Light olefins are important building blocks for many essential chemicals and products for industrial and domestic consumption, among which ethylene and propylene are the two most important light olefins [1,2]. At present, ethylene and propylene are mainly produced by the processes of naphtha cracking, MTO (methanol to olefins) and MTP (methanol to propylene, an on-purpose technology for producing propylene). In these processes, cryogenic distillation separation technology is applied, which is generally operated at temperatures as low as −100 °C; moreover, special cryogenic steels are required for constructing the distillation columns. Therefore, the cryogenic distillation process is very energy and capital intensive [3,4].

Due to the similar physical and chemical properties of ethylene and propylene, effective techniques for their separation are limited [5,6]. Membrane separation is generally considered to be energy efficient and environmentally friendly for gas separation [7-10]. In the cryogenic distillation separation process for olefins applied in industry today, a mixture of ethylene and ethane and a mixture of propylene and propane are separated from the product mixture, respectively, and then the desired ethylene and propylene are further separated from the ethane and propane. Ethane and propane are put together with other alkanes in the products and then combusted [11,12]. Based on the cryogenic distillation procedure, the separation of ethane from propane is unnecessary and more focus should be placed on the separation of ethylene from propylene in the membrane separation process. So far, the separation of ethylene/propylene by membranes is seldom reported in the literature, while the separation of olefins/paraffins by membranes has been extensively researched. From the literature for the separation of olefins and other gases with membranes [13-19], we can search for clues for membranes that have the potential to separate a propylene/ethylene mixture. 6FDA-Durene polyimide membranes have been used to investigate C_3H_6 and C_2H_4 pure gas permeation. The ideal C_2H_4/C_3H_6 selectivity is approximately 1.8 at 35 °C and 0.2 MPa [20]. Polydimethylsiloxane (PDMS) membranes [21], polyurethane-poly(vinylidene fluoride) (PU-PVDF) membranes [22], and poly (ethylene oxide) (PEO) membranes [23] have been applied for olefin/nitrogen or olefin/paraffin separation. On the basis of the pure gas permeability of propylene and ethylene in these membranes, the ideal C_3H_6/C_2H_4 selectivity ranges from 3.69 to 5.45 at 20 °C and 0.2 MPa. Under the same conditions, PEBA 2533, a commercial block copolymer composed of soft polyether (PE) amorphous segments and hard polyamide (PA) crystalline segments, shows a bigger ideal C_3H_6/C_2H_4 selectivity of 10.9 [18]. Therefore, PEBA2533 is advantageous in separating a propylene/ethylene mixture compared with reported materials.

Polymeric membranes used for gas separation often suffer from a "trade-off" phenomenon between membrane permeability and selectivity [24,25]. In particular, an increase in membrane permeability is often accompanied by a decrease in membrane selectivity

†To whom correspondence should be addressed.
E-mail: wangxiaodong@tyut.edu.cn, huangwei@tyut.edu.cn

or vice versa. To improve both the permeability and selectivity simultaneously, several strategies have been put forward, such as cross-linking modifications [10,26], polymer blends [27], and synthesis of mixed matrix membranes (MMMs) [28,29]. MMMs have drawn more attention because they exhibit the combined benefits of polymeric matrixes and inorganic additives. Polymeric matrixes have the advantage of processability and low cost while inorganic additives possess high permeability and selectivity [30]. The inorganic additives generally incorporated into polymeric matrixes for the fabrication of MMMs include carbon nanotubes [31-33], silica [34,35], MgO [36], polyhedral oligomeric silsesquioxane (POSS) [37], MOFs [20,28], zeolites and other nanoparticles [13,38-43]. Both 4A and NaY zeolites have stronger polarity, so introducing them into polymeric matrixes favors the separation of easily polarized gaseous molecules from a mixture. Incorporation of 4A zeolite into PEBA 1657 not only increases the membrane permeability for CO_2, CH_4, O_2, and N_2 but also increases the ideal selectivity for CO_2/CH_4 and O_2/N_2 [38]. Ahmad et al. studied the pure gas permeability of O_2, N_2, H_2 and CO_2 on poly(vinyl acetate)/4A MMMs and showed an enhanced ideal selectivity for O_2/N_2, H_2/N_2 and CO_2/N_2 gas pairs with increasing amount of zeolite grains in the membrane until up to 25 wt% [39]. Sanaeepura et al. [40] fabricated cellulose acetate/Co(II)-NaY MMMs and obtained remarkably enhanced CO_2 permeability and CO_2/N_2 selectivity on membranes compared with pure cellulose acetate membranes. The CO_2 permeability and CO_2/N_2 selectivity was increased by 43.9% and 61.7%, respectively.

Since ethylene molecules are symmetrical and nonpolar but propylene molecules are asymmetric and polar, it seems reasonable to take advantage of the polarity of NaA and NaY zeolites to improve the performance of polymeric matrixes in propylene/ethylene separation. It is anticipated that propylene will be preferentially adsorbed onto the zeolite grains from a mixture of ethylene and propylene, which favors selective permeation of propylene over ethylene. In the present work, we fabricated a series of MMMs (PEBA2533/NaA and PEBA2533/NaY membranes) and tested the separation of propylene from ethylene on the membranes. We investigated in detail the effects of the zeolite kind and amount of zeolite grains embedded in the membrane on the microstructure and separation performance of the membrane. In addition, the effect of operating conditions (i.e., temperature, pressure and composition of the gas mixture) on the membrane separation performance was also studied.

EXPERIMENTAL

1. Materials

PEBA 2533 polymer in the form of elliptic pellets was purchased from Arkema Inc. This polymer was comprised of 20 wt% poly [imino (1-oxodo-decamethylene)] as the amide segments and 80 wt% poly (tetramethylene oxide) as the ether segments. Silica sol (40 wt%) and 4A zeolite particles were supplied by Sigma-Aldrich and Energy Chemicals, respectively. Sodium hydroxide (NaOH) (A.R., >96 wt%) and sodium metaaluminate ($NaAlO_2$) were purchased from Kermel Co. and Sinopharm Chemical Reagent Co. respectively. N,N-dimethyl acetamide (DMAc) supplied by Aldrich was used during membrane preparation. All gases used in the experiments were of research grade (99.8-99.999% pure) and acquired from Taiyuan Iron and Steel Group Co., Ltd.

2. Membrane Preparation

First, the synthesis of nanosized NaY molecular sieves followed the hydrothermal process reported in the literature [44]. An aluminosilicate gel was prepared using silica sol as the silicon source, sodium metaaluminate ($NaAlO_2$) as the aluminum source and sodium hydroxide (NaOH) as the alkali source. Then, 3 g of $NaAlO_2$ was added to 43 ml of NaOH aqueous solution (3.4 M), followed by stirring for approximately 10 min. After that, 27.44 g of silica sol (40 wt%) was added to the mixture under stirring at ambient temperature and maintained at that temperature for 2 h to form the synthesis gel. The zeolite synthesis gel had a composition (in molar ratio) of 10 SiO_2 : Al_2O_3 : 5 Na_2O : 180 H_2O. The gel was transferred to a stainless-steel crystallization reactor and the crystallization reaction was allowed to occur at 100 °C for approximately 9 h. Then, the reactor was cooled to room temperature. The obtained suspension was centrifuged and rinsed thoroughly with deionized water until it became neutral. The obtained NaY crystal grains were dried at 60 °C and stored in a desiccator. After heating at 140 °C for 3-5 h to remove vapors adsorbed by the zeolite, the zeolite particles were imbedded into the polymeric matrix to synthesize MMMs.

PEBA2533/NaY membranes were prepared via the solution-casting technique. A predetermined amount of zeolite particles was dispersed in DMAc solvent to form a zeolite slurry, followed by sonication in an ultrasonic bath for 1 h to break up any aggregates of the particles. At the same time, sonication drove the particles to disperse more homogeneously in the suspension. Then, PEBA 2533 polymer pellets were added to the slurry under continuous agitation for 24 h at 70 °C. The solution was allowed to stand without disturbance for at least one day at 70 °C to remove gas bubbles. The solution was then cast onto a clean and dry glass plate to obtain the wet membranes, followed by evaporation of the solvent in a vacuum oven at 70 °C for one day to obtain PEBA2533/NaY membranes. The PEBA2533 polymer concentration in the slurry was kept at 15 wt%, whereas the concentration of zeolite NaY in the membrane casting slurry was predetermined so that the zeolite content in the resulting membranes was in the range of 0 to 10 wt%.

A similar procedure was used to prepare PEBA2533/NaA membranes, and the concentration of 4A zeolite in the membranes varied from 0 to 20 wt%.

3. Characterization

The crystal structure of zeolite NaY was measured by powder X-ray diffraction (XRD) using a Rigaku Miniflex 600 diffractometer employing Cu-K_α radiation at 40 kV and 20 mA, scanning over the range of 5-50° (2θ) at a rate of 4°/min.

The morphology of NaA and the as-synthesized NaY crystals was observed by a scanning electron microscope (SEM, JEOL JSM-6010PLUS/LV) at an accelerating voltage of 10-20 KV. The surface and cross-sectional morphology of the prepared PEBA2533/NaY membranes was examined using the same SEM. Homogeneous cross-sections of the samples were obtained by fracturing the samples in liquid N_2. The samples were sputter-coated at 10

mA for 60 s in a JEOL sputter coater fitted with Au. The thickness of the membranes was measured by using a Mitutoyo micrometer. The dispersion of the zeolite grains in the MMMs was detected by electron dispersive X-ray analysis (EDX, INCA-Oxford).

To detect the particle size distribution for the as-synthesized NaY, dynamic light scattering (DLS) analyses were performed at room temperature by utilizing a Malvern Zeta sizer Nano ZS90 particle size analyzer. The sample was sonicated in ethanol for 15 min to prepare a suspension. The counting rate for each measurement was kept at approximately 500 kcps with the results being averaged over at least three tests.

To investigate whether there was a chemical reaction between the NaY particles and the pure PEBA2533 molecules, attenuated total reflection Fourier-transform infrared (ATR-FTIR) spectra for as-synthesized NaY particles and PEBA2533/NaY MMMs were measured using an EQUINOX55 spectrometer (Bruker, Germany) over the wavenumber range from 400 cm^{-1} to 4,000 cm^{-1} at a resolution of 4 cm^{-1}.

4. Separation of Ethylene and Propylene Mixtures

Ethylene/propylene mixtures were separated using the as-synthesized PEBA2533/zeolite membranes as the separation materials with a constant-pressure and variable-volume method. The experimental setup used for ethylene/propylene separation by the membranes was the same as that shown elsewhere [18]. The olefin mixture was admitted to the membrane cell, which was placed in a thermal bath for temperature control. The effective membrane area for permeation was 12.56 cm^2. The quantity of the gas permeated through the membranes was measured using a homemade bubble flowmeter. The soap-bubble flowmeter mainly consists of a pipette (measurement range of 1 mL) and a glass junction, with an accuracy of 0.01 mL. The downstream composition of the gas was determined by a GC-950 gas chromatograph equipped with a thermal conductivity detector and an Agilent Porapak Q column. The membrane performance was evaluated in terms of permeability and selectivity. The permeability (P_A) of the membranes can be calculated using the following equation:

$$P_A = \frac{Q_A l}{At(p_1 - p_2)} \tag{1}$$

where Q_A is the quantity of the downstream gas A (cm^3(STP)), t is permeated time interval (s), A is the effective membrane area (cm^2), l is the thickness of the membrane (cm), p_1 and p_2 are the upstream and downstream partial pressures (cmHg), respectively. The permeability is usually expressed in barrer (1 barrer=10^{-10} cm^3(STP) cm/cm^2 s cmHg).

The mixed selectivity of gas A to gas B ($\alpha_{A/B}$), defined as their permeability ratio, was used to measure the membrane selectivity:

$$\alpha_{A/B} = \frac{P_A}{P_B} \tag{2}$$

where P_A and P_B represent the permeability of C_3H_6 and C_2H_4, respectively.

In the separation experiments for propylene/ethylene mixtures, the permeability and mixed gas selectivity of C_3H_6 to C_2H_4 were measured in the range of −35 °C to 20 °C and feed pressures ranging from 0.2 MPa to 0.5 MPa.

5. Adsorption Tests

The gas permeation through the membranes is believed to follow the solution-diffusion mechanism. Gas sorption in the zeolite fillers and in the membranes thus plays an important role in membrane permselectivity. The relationship between the solubility and the temperature for the two gases was determined using the pressure delay technique [45]. The sorption system consisted of two stainless steel chambers connected via a switching valve. One chamber is the sample chamber with a volume of 2.06 cm^3 (V_s), and the other chamber is a reference chamber with a volume of 4.73 cm^3 (V_R) (including associated connecting tubes).

The two chambers were kept at a constant temperature by a thermal bath. The gas pressure in the reference chamber was monitored by a pressure gauge. Membranes or zeolites of known volume were loaded into the sample chamber of the system, which was evacuated for approximately 3 h to remove the gas present in the system. Then, the sorbate gas was admitted to the pre-evacuated reference chamber until a given pressure (p_1) was reached. The gas stored in the reference chamber was allowed to flow to the sample chamber and the system was considered to be at sorption equilibrium after a constant pressure (p_2) was eventually reached. The quantity (mol) of the gas sorbed in the membranes or zeolite sorbents can be evaluated from

$$q_0 = \frac{(p_1 - p_2)V_R - P_2(V_s - V_m)}{RT} \tag{3}$$

where V_m is the volume of the membrane or zeolite sorbent sample (cm^3), and R and T are gas constant and operation temperature, respectively. Ideal gas behavior was assumed, which is reasonable for the relatively low pressures considered. After that, the connection between the two chambers was switched off and an additional amount of gas was admitted to the reference chamber to reach a pressure of p; then, a new sorption equilibrium was established at pressure p_e by connecting the two chambers. The incremental sorption uptake (mol) is given by

$$\Delta q = \frac{(p - p_e)V_R - (p_e - p_2)(V_s \mp V_m)}{RT} \tag{4}$$

Thus, the overall quantity of the gas sorbed in the sorbent at an equilibrium pressure of p_e is

$$q = q_0 + \Delta q = \frac{(p_1 - p_2 + p)V_R - p_e(V_R + V_s - V_m)}{RT} \tag{5}$$

In our experiment, p is always equal to p_1; Eq. (5) can be rearranged as follows:

$$q = q_0 + \Delta q = \frac{(2p_1 - p_2)V_R - p_e(V_R + V_s - V_m)}{RT} \tag{6}$$

The gas "solubility" in the sorbent characterized in terms of sorption uptake normalized by gas pressure is expressed as

$$S = \frac{q}{p_e} \tag{7}$$

In the experiment, the operation temperature varied from −15 °C to 20 °C.

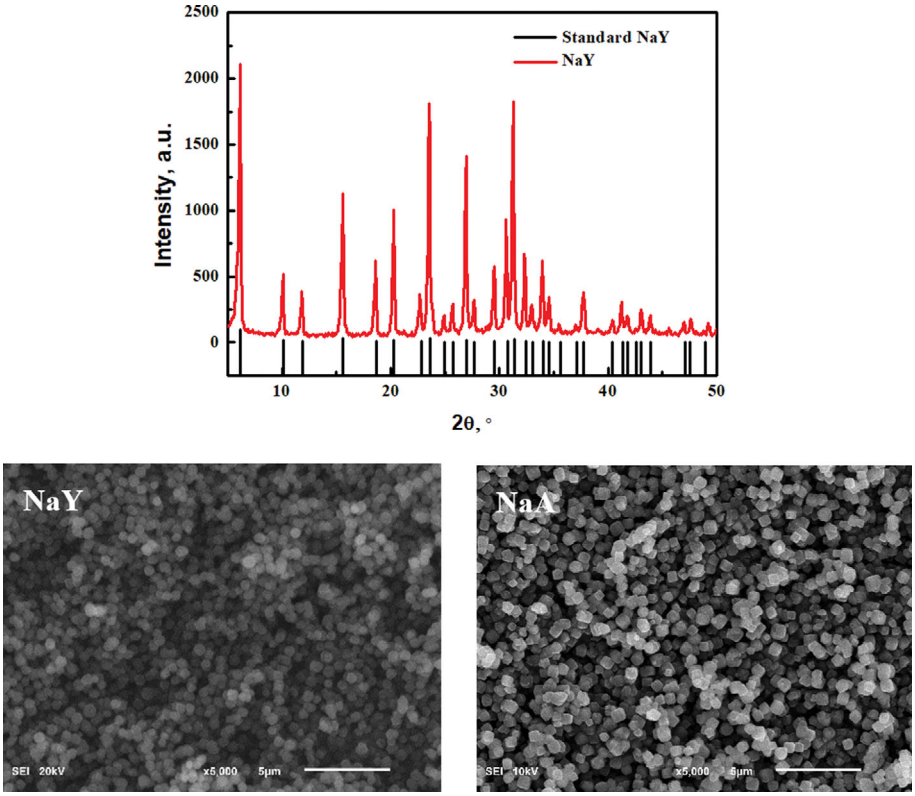

Fig. 1. X-ray diffraction patterns for zeolite NaY; SEM images of the zeolite NaY and NaA.

RESULTS AND DISCUSSION

1. Characterization

The XRD pattern for the synthesized NaY zeolite powders was detected to determine its topology, and the result is given in Fig. 1. As shown in Fig. 1, the as-synthesized NaY crystals show an XRD pattern that is well consistent with that given for standard NaY in the literature [46]. No diffraction peaks attributed to other crystals were observed. The SEM images show that both NaY and NaA crystals are uniform with a size of approximately 500-600 nm, and no amorphous staff is observed.

Fig. 2 displays the particle size distribution for the as-synthesized NaY zeolite characterized by DLS. The polydispersity index (PI) was found to be 0.316, which indicates that the particle size is well controlled [47]. The mass median diameter was determined to be 410 nm by the aforementioned method. The DLS result is consistent with that observed from SEM.

The main functional surface features for the as-synthesized NaY

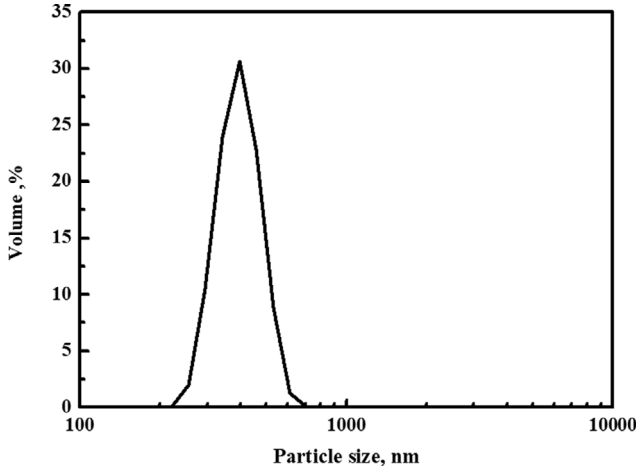

Fig. 2. Particle size distribution of as-synthesized NaY zeolite.

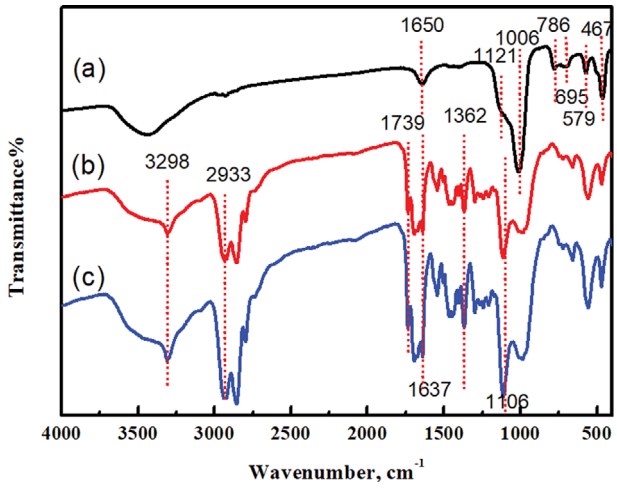

Fig. 3. ATR-FTIR spectra for as-synthesized NaY particles (a), pure PEBA2533 membrane (b) and PEBA2533/NaY-6 wt% MMMs (c).

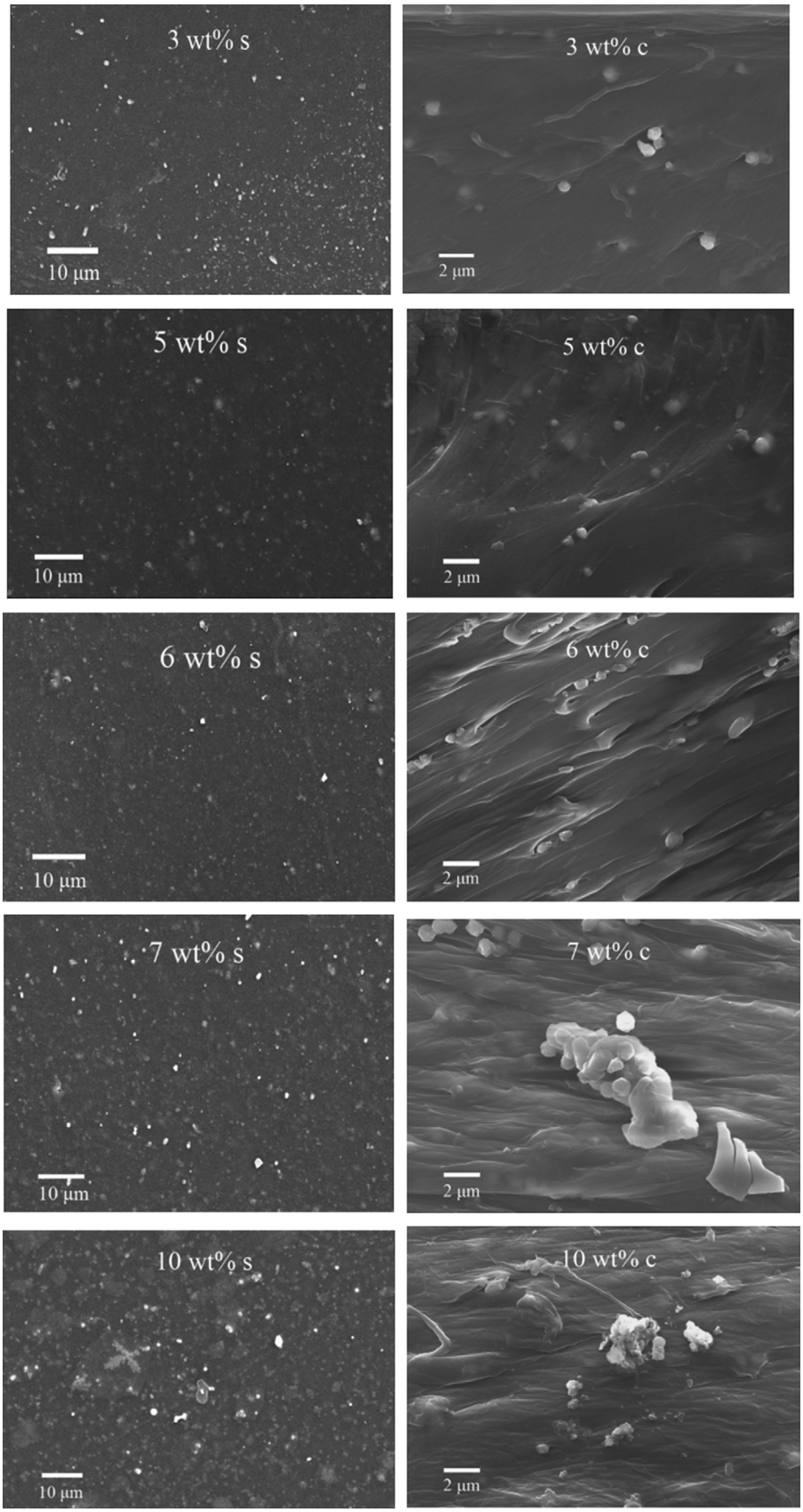

Fig. 4. SEM images of PEBA2533/NaY membranes containing different amounts of NaY grains (surface of the membranes is represented with s; cross-sections of the membranes are represented with c).

particles and fabricated membranes were characterized by ATR-FTIR. As expected, Fig. 3(a) shows the characteristic bands of zeolite Y. The band between 467 cm^{-1} and 506 cm^{-1} is assigned to T-O (T=Si or Al) symmetric stretching vibrations, while the band observed at 579 cm^{-1} arises from the presence of structural double rings (D6R) assigned to Y zeolite. The characteristic symmetric (695 cm^{-1}, 786 cm^{-1}) and asymmetric (1,006 cm^{-1}, 1,121 cm^{-1}) stretching vibrations are due to the [TO_4] tetrahedral blending band of the as-synthesized NaY sample [48]. The characteristic bands for PEBA2533 are shown in Fig. 3(b). The band at 1,106 cm^{-1} is the stretching vibration of C-O-C in the PE segment and the band at 3,298 cm^{-1} is ascribed to the N-H stretching vibration of the PA segment. The band at 1,739 cm^{-1} is assigned to the C=O stretching vibration of the carboxyl group that connects PA to the PE section [28]. Fig. 3(c) shows the ATR-FTIR spectrum for PEBA2533/NaY-6 wt% MMMs. It is obvious that Fig. 3(c) is the same as Fig. 3(b), which indicates that NaY crystal grains have only a physical reaction with PEBA2533 molecules and that no chemical reaction occurs between the two. All the NaY crystal grains are embedded into the inner region of the polymeric matrix and no crystals are located on the surface of the membrane because no characteristic bands for NaY zeolite are found in Fig. 3(c).

Fig. 4 shows SEM images of the surface and cross-section of PEBA2533/NaY membranes containing different amounts of NaY grains. All the membranes are dense and NaY crystal grains cannot be observed clearly on the surface of the membranes from the images of the surface, which is consistent with the ATR-FTIR result. The images of the cross-section of the membranes show that NaY

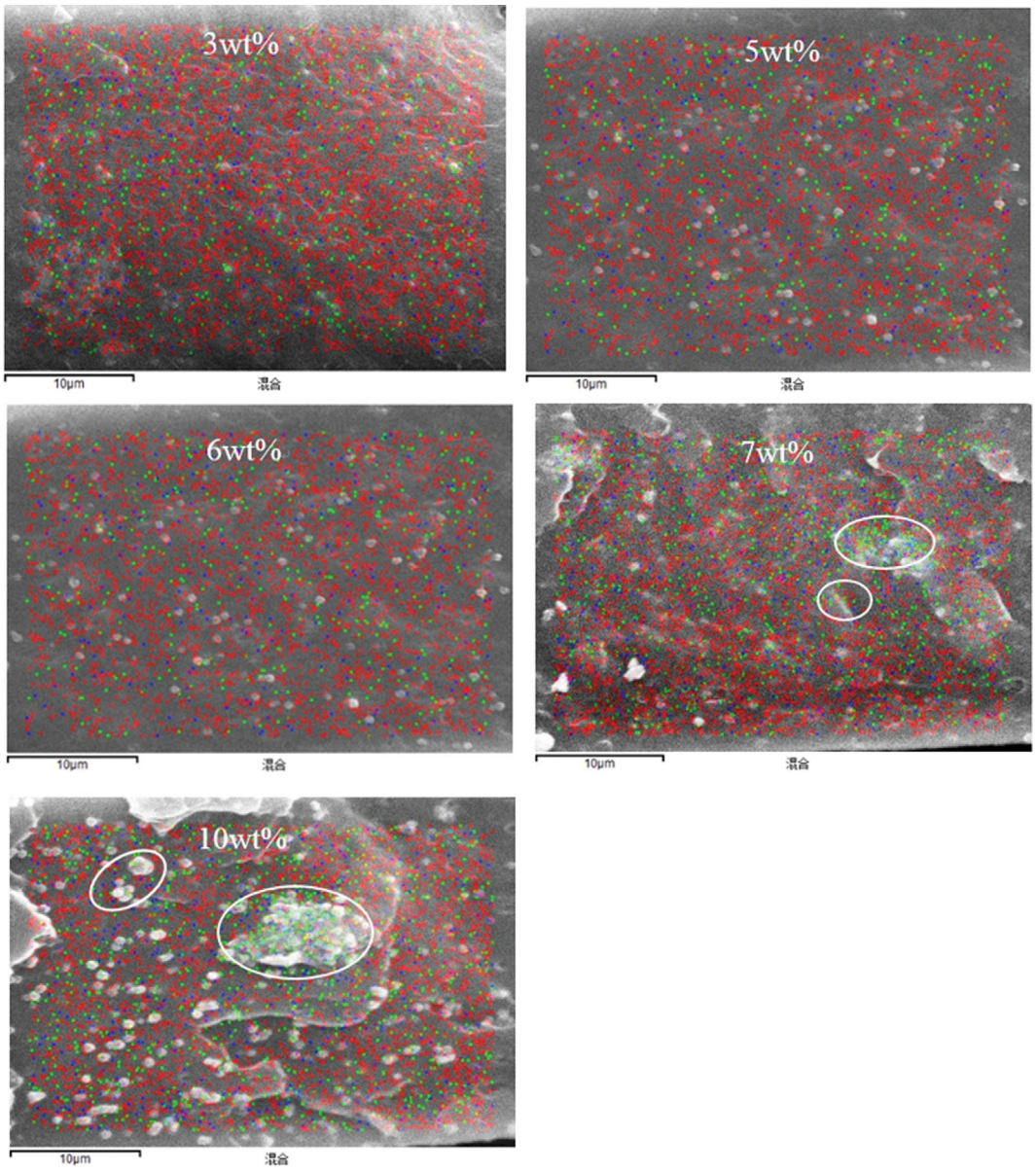

Fig. 5. SEM-EDX mapping images of cross-sections of PEBA2533/NaY membranes containing different amounts of NaY grains (C marked in red, Al marked in green, Si marked in blue).

crystals are uniformly dispersed in the polymer matrix at a content no greater than 6 wt.% and that further increasing the content (7 wt%-10 wt%) leads to gradual agglomeration of the zeolite crystals.

To further detect the distribution of NaY crystal grains in the polymeric matrix, SEM-EDX mapping images of the cross-sections of PEBA2533/NaY membranes containing different amounts of NaY grains were taken. The Al, Si and C elements were found to distribute uniformly in the membranes with a zeolite fraction of no greater than 6 wt%, as shown in Fig. 5. Upon increasing the amount of zeolite grains to 7 wt% and 10 wt%, Al becomes gradually non-uniform with intensive distribution in some section. This result reveals that zeolite grains are uniformly dispersed in the polymeric matrix when the NaY crystal fraction is no greater than 6 wt%, but with increasing zeolite content to 7 wt% and 10 wt%, the zeolite grains gradually agglomerate, consistent with the SEM result.

2. Mixed-gas Separation Performance

2-1. Selection of Additives

In this study, two kinds of additives were applied: NaY zeolite and NaA zeolite. To select the better additive, gas separation tests were carried out on the membranes containing different amounts of additives at −35 °C and 0.2 MPa using a propylene and ethylene mixture with a molar ratio of 50/50 as the feed gas. Fig. 6(a) shows the effect of NaY zeolite content (0 to 10 wt%) in membranes on the membrane separation performance. As the amount of NaY grains increases from 0 wt% to 6 wt%, the permeability of ethylene increases from 10 barrer to 31.2 barrer and that of propylene increases from 48 barrer to 211.3 barrer. The increase in propylene permeability is more significant than that in ethylene permeability, which gives rise to an increase in the selectivity of propylene to ethylene from 4.8 to 6.8. For a further increase in the amount of NaY grains to 10 wt%, the permeability of ethylene is enhanced from 31.2 barrer to 53.4 barrer and that of propylene from 211.3 barrer to 249.3 barrer. The more significant increase in ethylene permeability than propylene permeability leads to a decrease in the selectivity of propylene to ethylene from 6.8 to 4.7. Therefore, the membrane with 6 wt% NaY grains exhibits the best separation performance.

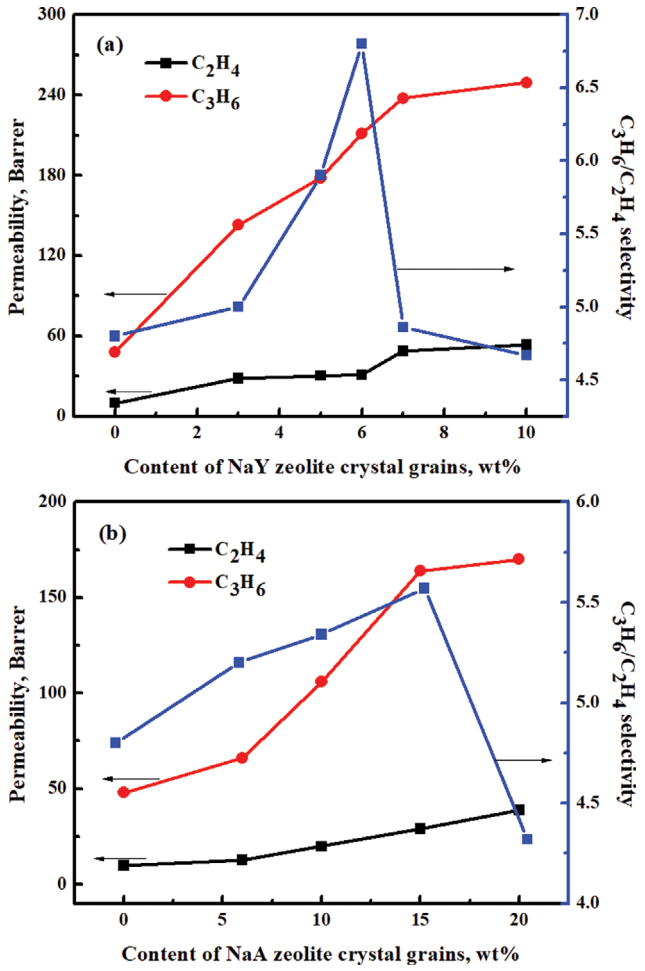

Fig. 6. Permeability and propylene/ethylene selectivity of membranes versus NaY zeolite content (a) and NaA zeolite content (b) in the membranes. Feed gas composition of propylene/ethylene (50/50, molar ratio); feed gas pressure of 0.2 MPa; operation temperature of −35 °C; membrane thickness of 65 μm.

Fig. 6(b) displays the ethylene and propylene separation performance for membranes containing different amounts of NaA zeolite (0 to 20 wt%) crystal grains. Similarly, the permeability of propylene increases faster than that of ethylene on the membranes containing NaA zeolite crystals with a fraction no greater than 15 wt%. However, the permeability of ethylene increases faster than that of propylene as the NaA zeolite crystal fraction further increases to 20 wt%. Based on the permeability, the membranes containing 15 wt% NaA grains were calculated to possess the biggest propylene/ethylene selectivity of 5.6 with a permeability of P_{C2H4}=29 barrer and P_{C3H6}=164 barrer in the series of membranes containing NaA zeolite.

From the observed separation performance on MMMs for an ethylene and propylene mixture, introducing NaY or NaA zeolite into PEBA2533 matrix improved the gas permeability and mixed gas selectivity simultaneously, and that NaY zeolite is more efficient as a filler. Generally, the gas transport in dense membranes follows the solution-diffusion mechanism [49,50]. The permeability P is described with P=D·S, where D is the diffusivity and S is the solubility. Polar zeolite NaY and NaA have a strong affinity for gas molecules. With the assistance of the polar zeolite grains, the solubility of the two kinds of gases studied in the MMMs is enhanced, as shown in the adsorption test (Fig. 7). In addition, the porous microstructure of zeolite crystals favors transport of the gas molecules through the membranes. These factors give rise to simultaneous improvement of the gas permeability and mixed gas selectivity. However, when the zeolite content is sufficiently high, the particle agglomeration, as shown by SEM and EDX results, deteriorates the interface between the polymer and the zeolite particles, which results in a reduction in the membrane selectivity. Thus, there exists an optimal amount of zeolite grains to improve the separation performance of the MMMs. The greater solubility (q/p_e) ratio of pure propylene to ethylene on NaY zeolite than that on NaA shown in Fig. 7 indicates that NaY zeolite is better than NaA zeolite as a filler. In the following studies, PEBA2533/NaY membranes were investigated to obtain insight into the membrane separation performance.

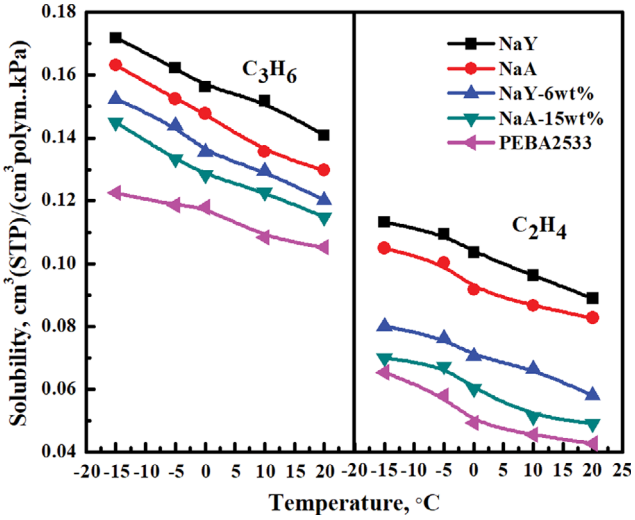

Fig. 7. Solubilities of pure ethylene and propylene in the MMMs, pure PEBA2533 membrane, and NaY and NaA zeolite crystals. Feed pressure of 0.2 MPa; membrane thickness of 65 μm.

To confirm the gas solubility of pure ethylene and propylene in the MMMs, sorption tests were carried out. Sorption tests on the zeolite grains as well as the pure PEBA2533 membrane were also conducted to thoroughly understand the effect of zeolite grains on the solubility of the gases. The solubility of pure ethylene and propylene in NaY and NaA zeolite is greater than that in the pure PEBA2533 membrane, as shown in Fig. 7. As expected, MMMs with NaY and NaA zeolite grains show greater solubility for ethylene and propylene than the pure PEBA2533 matrix.

The solubility of propylene is greater than that of ethylene in all kinds of membranes and zeolite grains. This is due to the higher critical temperature of propylene, which ensures that propylene condenses more easily than ethylene [45]. In addition, PEBA2533 is a block copolymer comprised of soft polyether segments and hard polyamide segments [37]. The ether oxygen linkage in the polymer has a stronger interaction with propylene (polar gas molecule) than ethylene, which helps to increase the solubility of propylene in the membrane [51-53]. The strong polarity of zeolite NaY and NaA, which ensures that they both adsorb polar propylene molecules more strongly than nonpolar ethylene molecules, is another factor.

The solubility of pure ethylene and propylene on NaY is always more than that on NaA at different temperatures. Moreover, the solubility (q/p_e) ratio of pure propylene to ethylene on NaY zeolite is 1.59 and that on NaA is 1.55. The former is a little greater than the latter. As we anticipate, the membranes with NaY zeolite grains show a greater solubility (q/p_e) ratio for pure propylene to ethylene (2.4) than the membranes with NaA zeolite grains (2.2).

2-2. Effect of Membrane Thickness on the Separation Performance of PEBA2533/NaY Membranes

The thickness of the membranes has both positive and negative effects on the separation performance of the membranes. As shown in Fig. 8, on the one hand, increasing the membrane thickness can eliminate the defects in the membranes and thus increase the selectivity of the membranes. On the other hand, the thicker

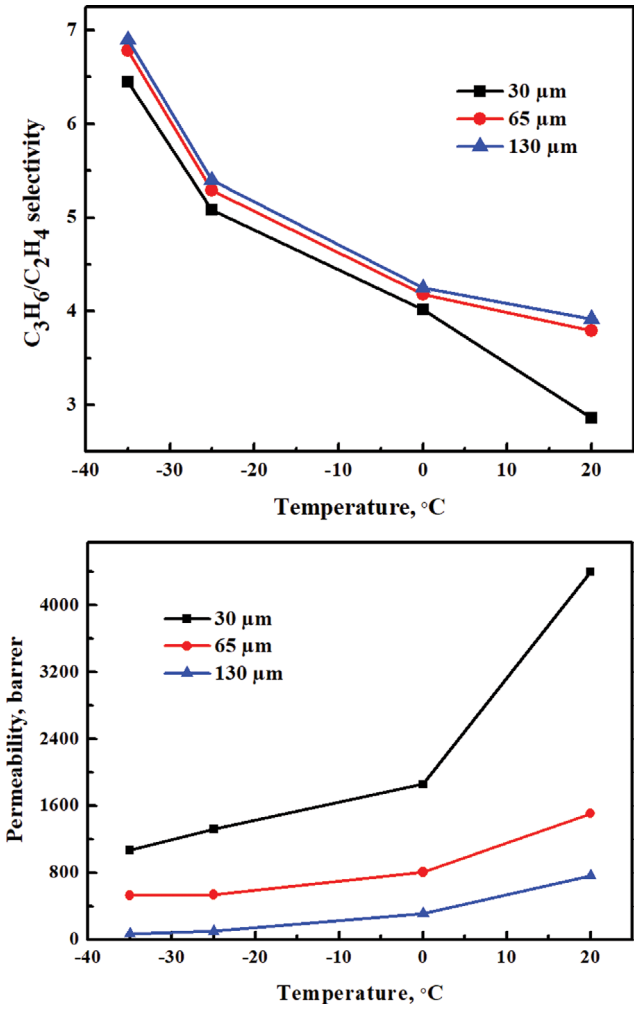

Fig. 8. Effect of membrane thickness on the separation of a propylene/ethylene mixture (50/50, molar ratio) by a PEBA2533/NaY-6 wt% membrane. The feed pressure is 0.2 MPa.

membranes show a smaller permeability. All the membranes mentioned above have a thickness of 65 μm. Upon decreasing the thickness to 30 μm, although the permeability of the PEBA2533/NaY-6 wt% membrane increases, the C_3H_6/C_2H_4 selectivity decreases from 6.8 to 6.3. When increasing the thickness to 130 μm, the C_3H_6/C_2H_4 selectivity (varying from 6.8 to 6.9) remains almost unchanged, while the permeability decreases significantly from 530 barrer to 72 barrer. Thus, for the PEBA2533/NaY-6 wt% membranes with a thickness of 65 μm, further increasing the thickness is not an efficient strategy to eliminate the defects in the membranes. Based on this, PEBA2533/NaY-6 wt% membranes with a thickness of 65 μm are used in the next study.

2-3. Effect of Operating Temperature and Pressure on the Separation Performance of MMMs

To study the effect of operating conditions on the membrane separation performance, the permeability and selectivity of MMMs were tested at different operation pressure and temperature. To ensure that the gas does not liquefy in the separation process, the saturated vapor pressure of the gas at different temperatures was calculated using the Antoine equation [54,55]:

$$\ln P = A - \frac{B}{T + C'}$$

where P is the saturated vapor pressure (mmHg), T is the temperature (°C), and A, B, and C are the Antoine constants. The Antoine constants for propylene are A=5.9445, B=785.85 and C=247, and those for ethylene are reported to be A=5.87246, B=585 and C=255 [56]. On the basis of a calculation, the operating temperature was determined to range from −35 °C to 20 °C, −25 °C to 20 °C, and 0 °C to 20 °C at 0.2 MPa to 0.3 MPa, 0.4 MPa, and 0.5 MPa, respectively. As shown in Fig. 9(a), the permeability of ethylene and propylene in the MMMs increases with increasing operating temperature. This is because an increase in temperature facilitates the thermal motion of the polymer chains, making it easier for the gas molecules to diffuse into the membrane. On the other hand, the gas molecules are more energetic at higher temperatures. Because propylene molecules are larger than ethylene molecules, increasing the temperature facilitates ethylene to diffuse into the membranes more remarkably than propylene. Indeed, the C_3H_6/C_2H_4 selectivity for MMMs is observed to decrease with increasing operating temperature, as shown in Fig. 9(b).

For the PEBA2533/NaY-6 wt% membrane, the permeability of ethylene and propylene in the MMMs increases when increasing the operating pressure, as shown in Fig. 9(a). According to Henry's law [57] (P_i=H·x_i, where P_i is the partial pressure of component *i*, H is Henry's constant and x_i is the molar fraction of the component *i* in the solvent), increasing operating pressure improves the solubility of propylene and ethylene in the membrane, and the greater solubility of the gases leads to a higher mobility of the polymer chains, which ensures that the gas diffuses more easily in the membrane.

However, the C_3H_6/C_2H_4 selectivity is reduced when increasing the operating pressure, as shown in Fig. 9(b). Increasing operating pressure indicates a bigger driving force, which has a more remarkable function on the smaller ethylene molecules [45,58]. For comparison, under optimum operating pressure (0.2 MPa), the performance of the PEBA2533/NaA-15 wt% membrane for separation of C_3H_6/C_2H_4 was also studied at an operating temperature ranging from −35 °C to 20 °C. The permeability of propylene on the PEBA2533/NaA-15 wt% membrane increases from 164 barrer to 490 barrer and that of ethylene increases from 29 barrer to 141 barrer, respectively. However, the C_3H_6/C_2H_4 selectivity decreases from 5.6 to 3.5. Under the same conditions, the permeability of propylene on the PEBA2533/NaY-6 wt% membrane increases from 213 barrer to 765 barrer and that of ethylene increases from 31 barrer to 202 barrer, respectively. Similarly, the C_3H_6/C_2H_4 selectivity decreases from 6.8 to 3.8. It is obvious that the PEBA2533/NaY-6 wt% membrane possesses both higher permeability and greater C_3H_6/C_2H_4 selectivity than the PEBA2533/NaA-15 wt% membrane at temperatures ranging from −35 °C to 20 °C.

2-4. Effect of the Gas Mixture Composition on the Separation Performance of the PEBA2533/NaY-6 wt% Membrane

From Fig. 10, it can be observed that as the propylene concentration in the gas mixture ranges from 10 mol% to 80 mol%, the C_3H_6/C_2H_4 selectivity increases from 2.3 to 13.1, respectively. When the propylene concentration is as low as 10 mol%, the membrane

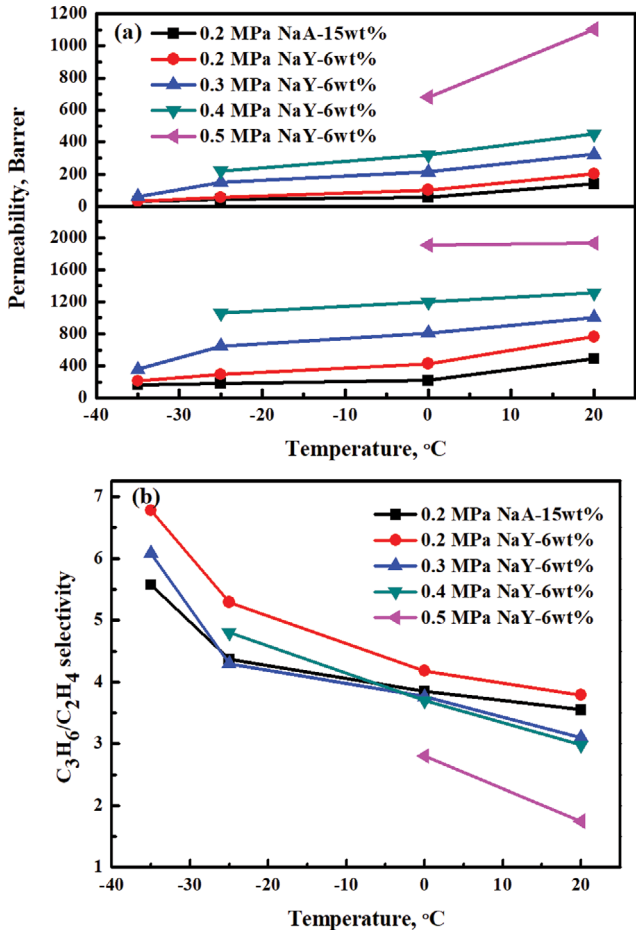

Fig. 9. Effect of operating temperature and pressure on the permeability (a) and propylene/ethylene selectivity (b) of a propylene/ethylene mixture (50/50, mola ratio) by MMMs (with NaY-6 wt% or NaA-15 wt%). Membrane thickness is 65 μm.

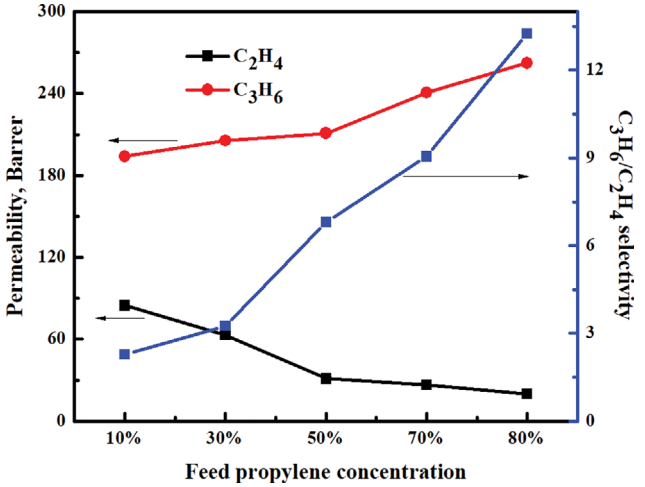

Fig. 10. Effect of the gas mixture composition on the separation performance of the PEBA2533/NaY-6 wt% membrane. Feed pressure is 0.2 MPa; temperature is −35 °C; membrane thickness is 65 μm; the propylene concentration in the feed gas mixture ranges from 10 mol% to 80 mol%.

Table 1. C_3H_6 and C_2H_4 permeation performance of different polymer membranes

Membrane	P (MPa)	T (°C)	C_3H_6/C_2H_4 (mol%)	P_{C2H4} (barrer)	P_{C3H6} (barrer)	$\alpha_{C3H6/C2H4}$	Ref.
PEBA2533/NaY	0.2	−35	50/50	31	213	6.87	This work
PEBA2533/NaY	0.2	−35	80/20	20	262	13.10	This work
PEBA2533/NaY	0.2	20	50/50	201	765	3.81	This work
PEBA2533	0.2	20	50/50	101	176	1.74	This work
PEBA2533	0.2	20	Pure gas	55	300	5.45[b]	[45]
PEBA2533/$AgBF_4$(0)	0.45	22	Pure gas	20[a]	110[a]	5.50[b]	[59]
PEBA2533/$AgBF_4$(20)	0.45	22	Pure gas	5[a]	45[a]	9.00[b]	[59]
PEBA2533/$AgBF_4$(40)	0.45	22	Pure gas	6[a]	10[a]	1.66[b]	[59]
PDMS	0.3	25	Pure gas	2,300	8,500	3.69[b]	[21]

[a]The unit is GPU, 1 GPU=3.35×10^{-10} mol/(m^2·s·Pa)
[b]The ideal selectivity

is not effective to separate propylene and ethylene. The permeability of propylene increases from 194 barrer to 262 barrer and that of ethylene decreases from 85 barrer to 19.8 barrer when the propylene concentration changes from 10 mol% to 80 mol%, respectively. From the perspective of the driving force for permeation, a rise in propylene concentration leads to an increase in the propylene partial pressure, resulting in an increase in the driving force for propylene, while for ethylene, the driving force decreases.

2-5. Comparison of the Results Obtained with those from other Similar Research

The separation of an ethylene and propylene mixture by membranes has not been reported so far to our knowledge. However, the permeation of pure propylene and ethylene on polymer membranes has been investigated [21,45,59]. Based on the pure gas permeability of ethylene and propylene in these membranes, the ideal selectivity can be calculated from the permeability ratio for propylene and ethylene. For comparison, the ideal selectivity and permeability for propylene and ethylene in polymer membranes reported in the literature are listed in Table 1. It is observed that the mixed gas selectivity is obviously lower compared to the ideal selectivity on PEBA2533 at 20 °C and 0.2 MPa. This is attributed to the plasticization of propylene in PEBA2533 membranes, which leads to a higher mobility for polymer chains and produces more free volume in the membrane. Thus, the diffusion of the smaller gas molecules of ethylene in the membrane is easier. It is also observed in other gas separation studies that the mixed gas selectivity is lower than the ideal selectivity on polymer membranes based on a solution-diffusion mechanism. Although it is difficult to compare the performance of the membranes exactly due to the different operation conditions employed in the literature, it can be seen that PEBA2533/NaY has an advantage compared with other membranes.

CONCLUSIONS

MMMs with different kinds of zeolite (NaY or NaA) were successfully fabricated by the casting method, and the synthesized membranes were used to separate a propylene/ethylene mixture. Incorporation of NaY or NaA zeolite into a PEBA 2533 matrix improved the propylene and ethylene separation performance significantly. As an inorganic additive, NaY zeolite was found to be more efficient than NaA zeolite because the former had a higher solubility for propylene and ethylene. Upon increasing the zeolite content in the membrane, the permeability of both propylene and ethylene increased, while the C_3H_6/C_2H_4 selectivity initially increased, and then decreased because of aggregation of the zeolite grains. The thinner the membranes, the larger the permeability. The C_3H_6/C_2H_4 selectivity was significantly increased as the thickness of the membranes was increased from 30 μm to 65 μm, but the mixed gas selectivity remained almost unchanged when the thickness was further increased to 130 μm. A lower operating temperature (−35 °C) and pressure (0.2 MPa) favors the selectivity of propylene to ethylene, while such conditions are adverse to the permeability of both gases. Using the highest quality membrane synthesized as the separation membrane (containing 6 wt% NaY with a thickness of 65 μm), when the propylene concentration was increased from 10 mol% to 80 mol% at −35 °C and 0.2 MPa, the propylene/ethylene selectivity was increased from 2.3 to 13.1, with the permeability of propylene increased from 194 barrer to 262 barrer and that of ethylene decreased from 85 barrer to 19.8 barrer, respectively. Finally, the incorporation of zeolite grains into a polymer matrix is an effective method to improve the separation performance of membranes, and this work will push forward the membrane separation process for olefin production.

ACKNOWLEDGEMENTS

The authors gratefully acknowledge the financial support from the Key projects of the National Natural Science Foundation of China (No. 21336006), the Scientific Research Foundation for Returned Scholars of Ministry of Education (No. 2017-047), the Foundation of State Key Laboratory of High-efficiency Utilization of Coal and Green Chemical Engineering (No. 2017-K15).

REFERENCES

1. R. Faiz and K. Li, *Desalination*, **287**, 82 (2012).
2. L. Li, R. B. Lin and R. Krishna, *Sicence*, **362**, 443 (2018).
3. W. Fan, X. Wang and X. Zhang, *ACS Cent. Sci*., **5**, 1261 (2019).

4. Z. Jingsheng and L. I. Dongfeng, *Chem. Ind. Eng. Prog.*, **34**, 3207 (2015).
5. C. A. Grande, C. Gigola and A. E. Rodrigues, *Ie&EC Process Des. Dev.*, **41**, 85 (2016).
6. H. Wu, Y. Chen and D. Lv, *Sep. Purif. Technol.*, **212**, 51 (2019).
7. L. Yu, M. Grahn and P. Ye, *J. Membr. Sci.*, **524**, 428 (2017).
8. R. W. Baker and B. T. Low, *Macromolecules*, **47**, 6999 (2014).
9. Y.-H. Chu, D. Yancey and L. Xu, *J. Membr. Sci.*, **548**, 609 (2018).
10. H. Sanaeepur, S. Mashhadikhan and G. Mardassi, *Korean J. Chem. Eng.*, **36**, 1339 (2019).
11. H.-J. Salgado-Gordon and G. Valbuena-Moreno, *CT&F, Cienc., Tecnol. Futuro*, **4**, 73 (2011).
12. Y. Wang, S. B. Peh and D. Zhao, *Small*, **15**, 1900058 (2019).
13. M. Naghsh, M. Sadeghi and A. Moheb, *J. Membr. Sci.*, **423-424**, 97 (2012).
14. C. Zhang, Y. Dai, and J. R. Johnson, *J. Membr. Sci.*, **389**, 34 (2012).
15. K. S. Liao, J. Y. Lai and T. S. Chung, *J. Membr. Sci.*, **515**, 36 (2016).
16. L. C. Mei, Y. Xiao and T. S. Chung, *Carbon*, **47**, 1857 (2009).
17. H. S. Kunjattu, V. Ashok and A. Bhaskar, *J. Membr. Sci.*, **549**, 38 (2017).
18. L. Li, A. Chakma and X. Feng, *J. Membr. Sci.*, **279**, 645 (2006).
19. J. J. Hou, P. C. Liu and Z. Y. Tang, *J. Mater. Chem. A*, **7**, 23489 (2019).
20. S. Japip, H. Wang and Y. Xiao, *J. Membr. Sci.*, **467**, 162 (2014).
21. S. H. Choi, J. H. Kim and S. B. Lee, *J. Membr. Sci.*, **299**, 54 (2007).
22. X. Jiang, J. Ding and A. Kumar, *J. Membr. Sci.*, **323**, 371 (2008).
23. H. Lin and B. D. Freeman, *J. Membr. Sci.*, **239**, 105 (2004).
24. L. M. Robeson, *J. Membr. Sci.*, **62**, 165 (1991).
25. L. M. Robeson, *J. Membr. Sci.*, **320**, 390 (2008).
26. B. Kraftschik and W. J. Koros, *Macromolecules*, **46**, 6908 (2013).
27. Y. Liu, S. Yu and H. Wu, *J. Membr. Sci.*, **469**, 198 (2014).
28. X. R. Zhang and T. Zhang, *J. Membr. Sci.*, **560**, 38 (2018).
29. L. Dong, C. Zhang and Y. Bai, *ACS Sustainable Chem. Eng.*, **4**, 3486 (2016).
30. Z. Farashi, S. Azizi and M. R.-D. Arzhandi, *J. Nat. Gas Sci. Eng.*, **72**, 103019 (2019).
31. M. N. Nejad, M. Asghari and M. Afsari, *ChemBioEng Rev.*, **3**, 276 (2016).
32. M. M. Khan, V. Filiz and G. Bengtson, *Procedia Eng.*, **9**, 1 (2014).
33. S. A. Habibiannejad, A. Aroujalian and A. Raisi, *RSC Adv.*, **6**, 79563 (2016).
34. J. Ahn, W. J. Chung and I. Pinnau, *J. Membr. Sci.*, **314**, 123 (2008).
35. S. M. Davoodi, M. Sadeghi and M. Naghsh, *RSC Adv.*, **6**, 23746 (2016).
36. C. H. Park, J. H. Lee and J. P. Jung, *J. Membr. Sci.*, **533**, 48 (2017).
37. M. Pazirofteh, M. Dehghani and S. Niazi, *J. Mol. Liq.*, **241**, 646 (2017).
38. R. S. Murali, A. F. Ismail and M. A. Rahman, *Sep. Purif. Technol.*, **129**, 1 (2014).
39. J. Ahmad and M. B. Hägg, *J. Membr. Sci.*, **427**, 73 (2013).
40. H. Sanaeepur, B. Nasernejad and A. Kargari, *Greenhouse Gases: Sci. Technol.*, **5**, 291 (2015).
41. Y. Dai, X. Ruan and Z. Yan, *Sep. Purif. Technol.*, **166**, 171 (2016).
42. I. Tirouni, M. Sadeghi and M. Pakizeh, *Sep. Purif. Technol.*, **141**, 394 (2015).
43. M. O. Najimu and I. H. Aljundi, *J. Nat. Gas Sci. Eng.*, **59**, 9 (2018).
44. L. Hu, Z. Zhang and S. Xie, *Catal. Commun.*, **10**, 900 (2009).
45. L. Liu, A. Chakma and X. Feng, *Chem. Eng. Sci.*, **61**, 6142 (2006).
46. N. J. Saleh, B. Y. S. Al-Zaidi and Z. M. Sabbar, *Arabian J. Sci. Eng.*, **11**, 5819 (2017).
47. B. A. Holmberg, H. Wang and J. M. Norbeck, *Micropor. Mesopor. Mater.*, **59**, 13 (2003).
48. S. Sang, Z. Liu and P. Tian, *Mater. Lett.*, **60**, 1131 (2006).
49. S. C. Feng, J. Z. Ren and K. S. Hua, *Sep. Purif. Technol.*, **116**, 25 (2013).
50. L. Dong, C. Zhang and Y. Bai, *RSC Adv.*, **5**, 4947 (2015).
51. V. I. Bondar, B. D. Freeman and I. Pinnau, *J. Polym. Sci., Part B: Polym. Phys.*, **38**, 2051 (2015).
52. J. H. Kim, S. Y. Ha and Y. M. Lee, *J. Membr. Sci.*, **190**, 179 (2001).
53. B. Wilks and M. E. Rezac, *Atmos. Chem. Phys.*, **85**, 2436 (2002).
54. K. Chatterjee, D. Dollimore and K. Alexander, *Int. J. Pharm.*, **213**, 31 (2001).
55. A. Hazra, D. Dollimore and K. Alexander, *Thermochim. Acta*, **392**, 221 (2002).
56. R. M. Stephenson and S. Malamowski, *AIChE J.*, **35**, 877 (1989).
57. R. Sander, *Atmos. Chem. Phys.*, **15**, 4399 (2015).
58. P. F. Nealey, R. E. Cohen and A. S. Argon, *Macromolecules*, **27**, 4193 (1994).
59. T. C. Merkel, R. Blanc and I. Ciobanu, *J. Membr. Sci.*, **447**, 177 (2013).